Improvement of Inversion Solutions of the Elliptic Cone Model for Frontside Full Halo CMEs

X. P. Zhao

W. W. Hansen Experimental Physics Laboratory,

Stanford University, Stanford, CA 94305-4085

Received _____; accepted _____

Submit to Astrophys. J., April 19, 2010

ABSTRACT

The elliptic model parameters inferred from the inversion equation system of the elliptic cone model in Zhao (2008) can be used to reproduce only a small part of frontsid full-halo CMEs that occured near the solar disk center. It is found that the phase angle advance of elliptic cone-base radius was set to increase clockwise and other angles involved in the model are counter-clockwise in Zhao (2008). By changing the setting from clocksise to counter-clockwise, a new inversion equation system of the elliptic cone model is derived. The inversion solutions obtained from the new inversion equation system can be used to well reproduce all ellipse-like fronside full halo CMEs.

1. Introduction

Coronal mass ejections (CMEs) are believed to be driven by the free magnetic energy stored in field-aligned electric currents, and the magnetic configuration of most, if not all, CMEs is thus expected to be CME ropes, i.e., magnetic flux ropes with two ends anchored on the solar surface (e.g. Riley et al., 2006). Most limb CMEs appear as planar looplike transients with a radially-pointed central axis and a constant angular width. The existence of full halo CMEs, i.e., those CMEs with an apparent (sky-plane) angular width of 360°, implies that the looplike transients are three-dimensional (Howard et al., 1982). Both looplike and halolike CMEs show the evidence of the CME rope configuration.

The bright structures characterizing coronal mass ejections (CMEs) observed by coronagraphs in the plane of sky are the photospheric light scattered by CME electrons along the line-of-sight. Outlines of many, if not most of, full halo CMEs are ellipse-like. A conical shell (or cone) model, i.e., a hollow body which narrows to Sun's spherical center

from a round, flat base was suggested to be similar to 3-D CME structures (Howard et al., 1982). The circular cone model has been used to infer geometrical and kinematical properties of 3-D CME ropes from observed apparent geometrical and kinematical properties of 2-D elliptic halo CMEs (Zhao et al., 2002; Xie et al, 2004).

Ellipse-like halo CMEs can be classified into Types A, B, and C based on whether the minor (Type A) or major (Type B) axis of ellipse-like halos passes through or not (Type C) the solar disk center, as shown in Figure 1 of Zhao (2008) (Zhao08, hereafter). It has been shown, however, that the circular cone model may be used to produce only Type A FFH CMEs and is not valid for Types B and C halo CMEs. (Zhao, 2005).

The outer boundary of the top (or leading) part of CME ropes may be better approximated by ellipses than circles. The elliptic cone model has been developed to invert the model parameters that characterize the propagation direction, size, shape and orientation of 3-D CME ropes [Zhao, 2005; Cremades and Bothmer, 2005]. We had established an inversion equation system for the elliptic cone model trying to invert the model parameters for all three types of ellipse-like CMEs (Zhao08). It is found, however, that the inversion equation system works only for Types A, B, and a small part of Type C halo CMEs of which the associated near-surface activity occurred near the solar disk center as shwon in Figures 6, 7, 8 of Zhao08.

It is found that the phase angle of radii of elliptic halos relative to SA_{yo} axis, δ_h, in Zhao08 was defined to increase clockwise and other angles used in Zhao08 increase counter-clockwise. This inconsistence is the cause of the failure in inverting model parameters for most Type C halo CMEs. By defining δ_h to increase counter-clockwise, the present paper establish an new inversion equation system so that the non-disk Type C FFH CMEs, as well as Types A, B, and disk Type C, can be more accurately reproduced using the inversion model parameters obtained from the new inversion equation system.

2. Expressions for modeled and observed halo CMEs

In the Heliocentric Ecliptic coordinate system $X_hY_hZ_h$, X_h axis points to the Earth, Y_h axis to the west, and Z_h axis is normal to the eclipse and points to the north. The plane Y_hZ_h represents the sky-plane where the halo CMEs occur due to the projection of the CME ropes. The propagation direction of the CME ropes (the direction of the central axis of the elliptic cone model) is assumed to be radial and is expressed by the sky-plane latitude β and longitude α in what follows, instead of the commonly used ecliptic-plane latitude and longitude.

2.1. Six model parameters and expressions for modeled halos

Elliptic cones can be expressed in the cone coordinate system $X_cY_cZ_c$ of which the origin is colocated with the origin of the $X_hY_hZ_h$ system. The X_c axis aligned with the central axis of the elliptic cone, and expressed by the sky-plane latitude and longitude, β, α. The sky-plane latitude β denotes the angle from the central axis X_c to its projection, X_c', in the plane Y_hZ_h (See the top-left panel of Figure 1), and the longitude α the angle from X_c' to the west axis Y_h (See the top-right panel of Figure 2), both increase counter-clockwise.

The base of elliptic cones is parallel to the the plane Y_cZ_c normal to the X_c axis (see Figure 1). The axis Y_c is the intersection between the plane Y_hZ_h and the plane Y_cZ_c. Four more model parameters, R_c, ω_y, ω_z, and χ are needed to characterize the elliptic cone base in $X_cY_cZ_c$ system. As shown in Figure 1, parameter R_c denotes the distance from Sun's spherical center to the center of the cone base; ω_y and ω_z are the half angular width covered by two semi-axes of elliptic bases, SA_{yb} and SA_{zb} respectively; χ is the angle from the semi-axis SA_{yb} to the Y_c axis.

Given a set of values for five model parameters R_c, ω_y, ω_z, χ, β, the projected base in

the plane $X'_cY'_c$ (See Figure 2) can be obtained by first trasforming the rim of the elliptic cone base to $X_cY_cZ_c$ and then from $X_cY_cZ_c$ to $X'_cY'_cZ'_c$ (see Zhao08 for the details),

$$\begin{bmatrix} x'_{cm} \\ y'_{cm} \\ z'_{cm} \end{bmatrix} = \begin{bmatrix} \cos\beta & \sin\beta\sin\chi & -\sin\beta\cos\chi \\ 0 & \cos\chi & \sin\chi \\ \sin\beta & -\cos\beta\sin\chi & \cos\beta\cos\chi \end{bmatrix} \begin{bmatrix} R_c \\ R_c\tan\omega_y\cos\delta_b \\ R_c\tan\omega_z\sin\delta_b \end{bmatrix} \quad (1)$$

where the symbol δ_b is the phase angle of radii of elliptic bases relative to SA_{yb} axis and increases counter-clockwise along the rim of the elliptic base from 0° to 360° (Note Expression (1) here slightly differs from Expression (5) in Zhao08 due to the typos existed in (5) there).

The modeled halo in the sky-plane Y_hZ_h can be obtained by rotating the projected base an angle of α around X_h axis (Figure 2).

$$\begin{bmatrix} y_h \\ z_h \end{bmatrix} = \begin{bmatrix} \cos\alpha & \sin\alpha \\ -\sin\alpha & \cos\alpha \end{bmatrix} \begin{bmatrix} x'_{cm} \\ y'_{cm} \end{bmatrix} \quad (2)$$

2.2. Five halo parameters and expressions for observed halos

As shown in Figure 2 for modeled halos and Figure 3 for observed halos, elliptic halos in Y_hZ_h plane can be characterized using five halo parameters: D_{se}, α, SA_{xo}, SA_{yo}, and ψ. Here D_{se} denotes the distance from solar disk center to halo center. The projection of the cone central axis (X_c) in the sky-plane, X'_c, is aligned with D_{se}. The axis Y'_c is in the Y_hZ_h plane and perpendicular to the D_{se} and thus aligned with Y_c axis. Parameter α is the sky-plane longitude as mentioned above. Parameters SA_{xo} and SA_{yo} are semi-axes of observed elliptic halos adjacent to X'_c and Y'_c respectively. Parameter ψ denotes the angle from axes SA_{yo} to Y'_c and increases counter-clockwise. Therefore, the five halo parameters characterize the location of the center (D_{se}, α), the size and shape (SA_{xo}, SA_{yo}) and the orientation (ψ) of ellipse-like halos. By using four halo parameters D_{se}, SA_{xo}, SA_{yo}, and ψ,

the 2-D elliptic halo in the plane $X'_cY'_c$ can be expressed

$$\begin{bmatrix} x'_{co} \\ y'_{co} \end{bmatrix} = \begin{bmatrix} D_{se} \\ 0 \end{bmatrix} + \begin{bmatrix} \cos\psi & \sin\psi \\ -\sin\psi & \cos\psi \end{bmatrix} \begin{bmatrix} -SA_{xo}\sin\delta_h \\ SA_{yo}\cos\delta_h \end{bmatrix} \tag{3}$$

The symbol δ_h in equation (3) is the phase angle of radii of elliptic halos relative to SA_{yo} axis, and increases counter-clockwise along the elliptic rim from 0° to 360° (Note: Expression (3) here differs from Equations (1) and (2) in Zhao08 because of different definition for the δ_h advance).

The observed halo in the sky-plane Y_hZ_h can be expressed by rotating the above ellipse in $X'_cY'_c$ an angle of α around X_h axis using the matrix in Equation (2).

3. Derivation of new inversion equation System

Since parameter α is both the model parameter and halo parameter, it is not necessary to include α in the following equation systems that associate model parameters with halo parameters.

In Equation systems (1) and (3), variables δ_b and δ_h vary, respectively, in the planes Y_cZ_c and $X'_cY'_c$. As shown by the black dots in the four panels of Figure 2, for unprojected (top left panel) and projected (other panels) cone base, the black dots are not the end-point of semi-major axis in the cases of projected bases, though it is the end-point of semi-major axis for the unprojected base. It shows that unless for the special cases of $\chi \simeq \psi \simeq 0$ or β is greater than 70°, $x'_{cm} \neq x'_{co}$ and $y'_{cm} \neq y'_{co}$ when $\delta_h = \delta_b$.

We assume that $x'_{cm} = x'_{co}$ and $y'_{cm} = y'_{co}$ when $\delta_h = \delta_b + \triangle\delta$,. By replacing δ_h in Equation (3) with $\delta_b + \triangle\delta$,, and comparing the like items between Equations (1) and (3), the relationship between elliptic cone model parameters and elliptic CME halo parameters

can be established

$$\begin{aligned} R_c \cos\beta &= D_{se} \\ R_c \tan\omega_y \sin\beta \sin\chi &= -SA_{xo} \cos\psi \sin \triangle\delta + SA_{yo} \sin\psi \cos\triangle\delta \\ R_c \tan\omega_z \sin\beta \cos\chi &= SA_{xo} \cos\psi \cos \triangle\delta + SA_{yo} \sin\psi \sin\triangle\delta \\ R_c \tan\omega_y \cos\chi &= SA_{xo} \sin\psi \sin \triangle\delta + SA_{yo} \cos\psi \cos\triangle\delta \end{aligned} \tag{4}$$

Five model parameters occur in left side of Equation system (4), and four halo parameters and the unknown parameter $\triangle\delta$ in right side. To find out the model parameters, the parameter $\triangle\delta = \delta_h - \delta_b$ must first be specified.

Since axis Y_c' is aligned with axis Y_c, the radii of modeled and observed halos are expected to meet at Y_c' when $\delta_b = \chi$ and $\delta_h = \psi$. The red dots in Figure 2, i.e., the end-point of the radius aligned with Y_c of the unprojected base projected cone bases does intersect with the end-point of the radius aligned with Y_c' axis when $\delta_b = \chi$, and $\delta_h = \psi$.

Thus we have $\triangle\delta = \delta_h - \delta_b = \psi - \chi$. By replacing $\triangle\delta$ in Equation system (4) with $\psi - \chi$, we have

$$\begin{aligned} R_c \cos\beta &= D_{se} \\ (R_c \tan\omega_y \sin\beta - a)\tan\chi &= -b \\ R_c \tan\omega_z \sin\beta - b\tan\chi &= a \\ R_c \tan\omega_y + b\tan\chi &= c \end{aligned} \tag{5}$$

where

$$\begin{aligned} a &= SA_{xo}\cos^2\psi + SA_{yo}\sin^2\psi \\ b &= (SA_{xo} - SA_{yo})\sin\psi\cos\psi \\ c &= SA_{xo}\sin^2\psi + SA_{yo}\cos^2\psi \end{aligned} \tag{6}$$

When $\omega_y = \omega_z$ (and thus $\chi = \psi = 0$), the number of model parameters equals the number of halo parameters, Equation system (5) reduce to the inversion equation system for the circular cone model (Xie et al., 2004).

The new inversion equation system for the elliptic cone model can be derived from Equation system (5)

$$\begin{aligned} R_c &= D_{se}/\cos\beta \\ \tan\omega_y &= [(a + c\sin\beta) \mp \sqrt{(a - c\sin\beta)^2 + 4\sin\beta\, b^2}\,]/(2R_c\sin\beta) \\ \tan\chi &= (c - R_c\tan\omega_y)/b \\ \tan\omega_z &= (a + b\,\tan\chi)/R_c\sin\beta \end{aligned} \tag{7}$$

Equation systems (6) and (7) here are different from Equation systems (9) and (11) in Zhao08.

4. Comparison of new with old inversion solutions

The inversion equation system (7) shows that if the sky-plane latitude β can be specified for a CME, the four unknown model parameters, R_c, ω_y, ω_z and χ, can be uniquely determined by coefficients a, b, and c. The coefficients a, b, and c can be calculated using Equation system (5) and observed four halo parameters, D_{se}, SA_{xo}, SA_{yo} and ψ (Figure.3).

Zhao08 suggested an approach, the one-point approach, to find out the candidate model parameter β for FFH CMEs. The approach is based on informations included in the disk location of associated flare and the measured parameter α (see Figure 3 for the four events). The candidate sky-plane latitudes β for the four Type C FFH CMEs in Figure 3 have been calculated in Zhao08 (See Section 5 of Zhao08 for the details).

Based on the same candidate sky-plane latitudes β and the same halo parameters, we calculate the four unknown model parameters for the four events in Figure 3 using the new inversion equation system (7). By inserting the newly obtained model parameters (see the green numbers in Figures 4 and 5) into Equation systems (1) and (2), the modeled halos are obtained, as shown by green ellipses in Figures 4 and 5. For comparison, the old results

in Zhao08 for the four Type C FFH CMEs are also shown in Figures 4 and 5 by red ellipses.

The white ellipses in Figures 4 and 5 are the outlines of observed FFH CMEs identified using the five-points method (See Cremade, 2005 for the details).

Figures 4 and 5 show that the green ellipses agree with the white ellipses much better than the red ellipses. All green ellipses agree with white ones equally well, no matter what value of β is. For the red ellipse, only the 20001124 event with β greater than 70° can approximately match the white ellipse.

5. Summary and discussion

By using the counter-clockwise definition for the angle advance of all kinds of angles involved in the elliptic cone model, we established the equation system (4) that relate five model with four halo parameters. Based on the characteristics of projected cone base relative to the unprojected cone base, we then determine $\triangle\delta = \delta_h - \delta_b = \psi - \chi$, and derive the new inversion equation system (7) for the elliptic cone model of halo CMEs.

The new inversion solutions obtained using the new inversion equation system can be used to very well reproduce all kinds of Type C halo CMEs, no matter what the disk location of the associated flare is. It shows significant improvement over the old solutions. Since Types A and B halo CMEs are the specific cases of Type C. The new inversion equation system should also work well for all three Types of halo CMEs.

A successful space weather forecasting depends on the successful simulation of CME propagation in the inner heliosphere. The later depends on the successful determination of the 3-D kinematic properties from the elliptic cone model based on the successful determination of (a) the outline of halo CMEs, (b) the sky-plane latitude β by one-point or two-point approach, (c) the geometric properties from the inversion equation system.

We have developed the algorithm for inverting 3-D kinematic properties on the basis of the newly inverted elliptic cone model parameters and the observed apparent 2-D kinematic properties of halo CMEs (Zhao, Cremades and Owens, 2010).

To validate the sky-plane latitude β obtained using one-point approach, we are analyzing the Febury 7, 2010 event simultaneously observed by SOHO/LASCO and COR1 and COR2 on STEREO a and B.

It is found that such inverted 3-D geometric properties are sensitive to the halo parameters determined on the basis of the identified elliptic outline of full-halo CMEs. It is necessary to more objectively recognize the outer edge of halo CMEs so that we can reduce or avoid fitting errors occured in the halo parameters.

The author thanks Hebe Cremades for providing the data files used in Figures 3, 4 and 5. This work is supported by NASA grants NAGW 2502 and NAG5-3077, by NSF grant ATM9400298.

REFERENCES

Cremades, H., 2005, *Ph. D. thesis, Copernicus GmbH, Katlenburg-Lindau, Germany, ISBN: 3-936586-40-3.*

Cremades, H. and V. Bothmer, 2005, in *Proc. IAL Symp. 226 on Coronal and Stellar Mass Ejections*, edited by K. P. Dere, J. Wang, and Y. Yan, IAU, Cambridge, 48.

Cremades, H. and V. Bothmer, Tripathi, D., 2006, *Adv. Space Res. 38*, 3, 461-465.

Howard, R. A., D. J. Michels, N. R. Sheeley Jr., and M. J. Koomen, 1982,

Riley, P., C. Schatzman, H. V. Cane, I. G. Richardson, N. Gopalswamy, 2006, *Astrophys. J., 647*, 648.

Xie, H., L. Ofman and G. Lawrence, 2004, *J. Geophys. Res.109, A03109, doi:10.1029/2003ja010226.*

Zhao, X. P., 2005, in *Proc. IAL symp. 226 on Coronal and Stellar Mass Ejections*, edited by K. P. Dere, J. Wang, and Y. Yan, IAU, Cambridge, 42.

Zhao, X. P., 2008, in *J. Geophys. Res.113, A02101, doi:10.1029/2007JA012582.*

Zhao, X. P. S. P. Plunkett and W. Liu, *J. Geophys. Res., 107, doi:10.1029/2001JA009143.*

Zhao, X. P., Cremades, H. and Owens, M. J., *prepared.*

This manuscript was prepared with the AAS LaTeX macros v5.2.

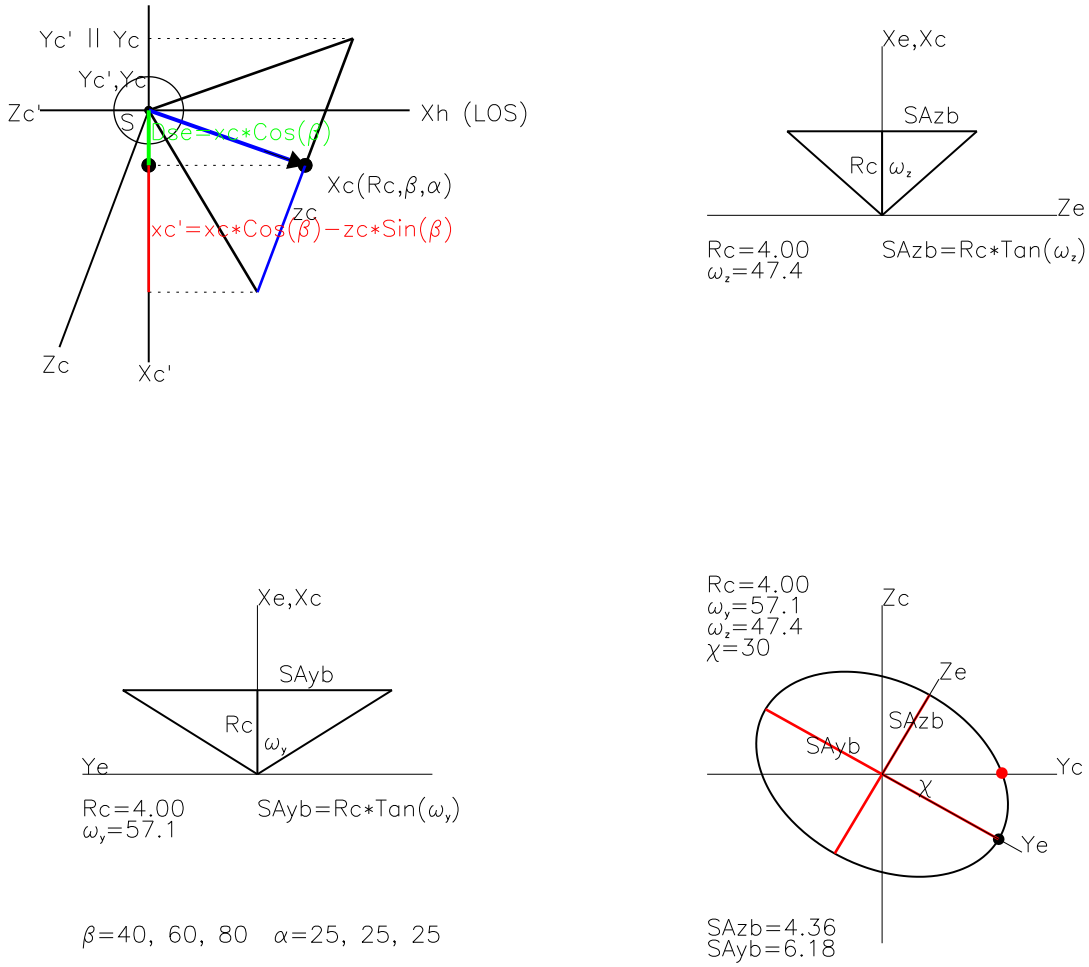

Fig. 1.— The top-left panel shows the relationship among coordinate systems $X_hY_hZ_h$, $X_cY_cZ_c$, and $X'_cY'_cZ'_c$. Axes X'_c, Y'_c, and Y_c are all located in the sky-plane Y_hZ_h that is normal to the axis X_h. The axis X_c denotes the direction of the central axis of the elliptic cone (β, α) and the distance of the cone base from the Sun's center (R_c). The other three panels show the definition of model parameters, ω_y, ω_z, and χ characrizing the elliptic cone base in the plane Y_cZ_c normal to X_c axis.

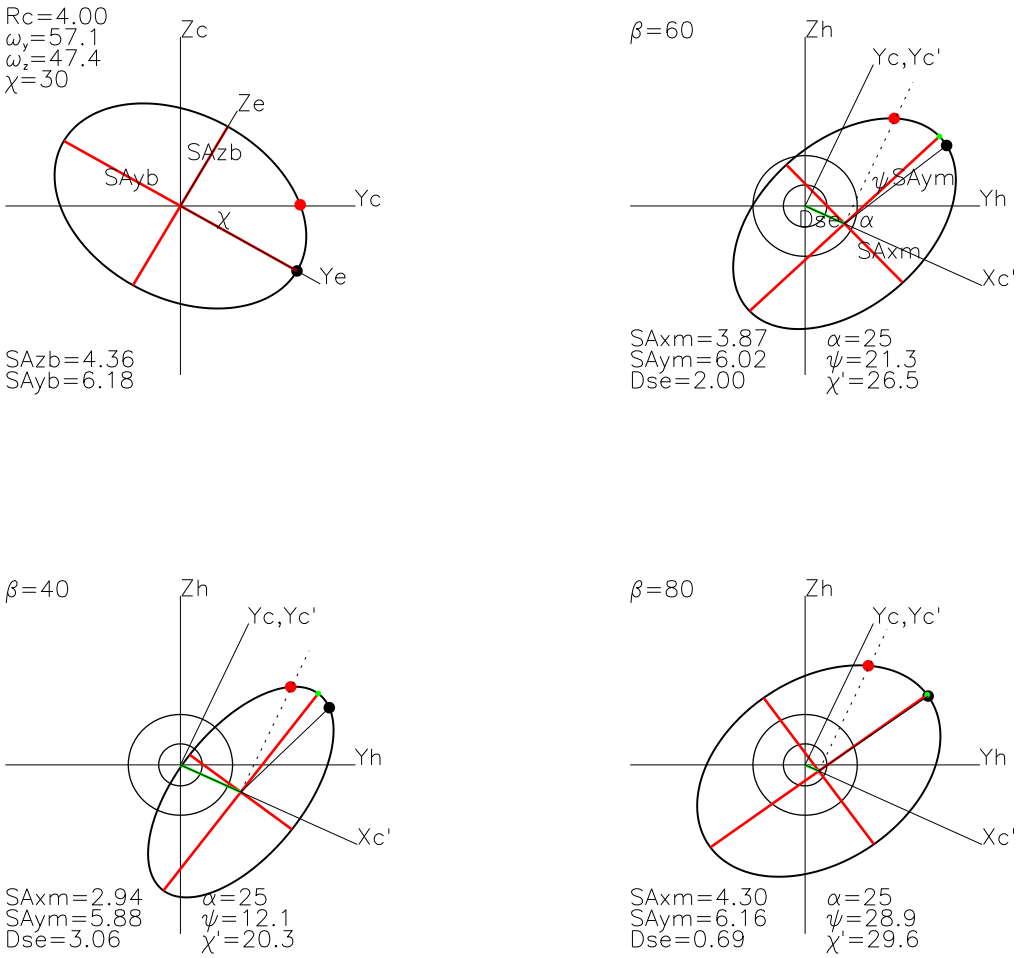

Fig. 2.— Projection of a cone base in Y_cZ_c (top-left panel) onto the sky-plane with $\beta = 40°, 60°, 80°$. The black and red dots denote, respectively, the end-point of unprojected base radii (top-left panel) and that of projected base radii (other panels) when $\delta_b = 0$ and $\delta_b = \chi$.

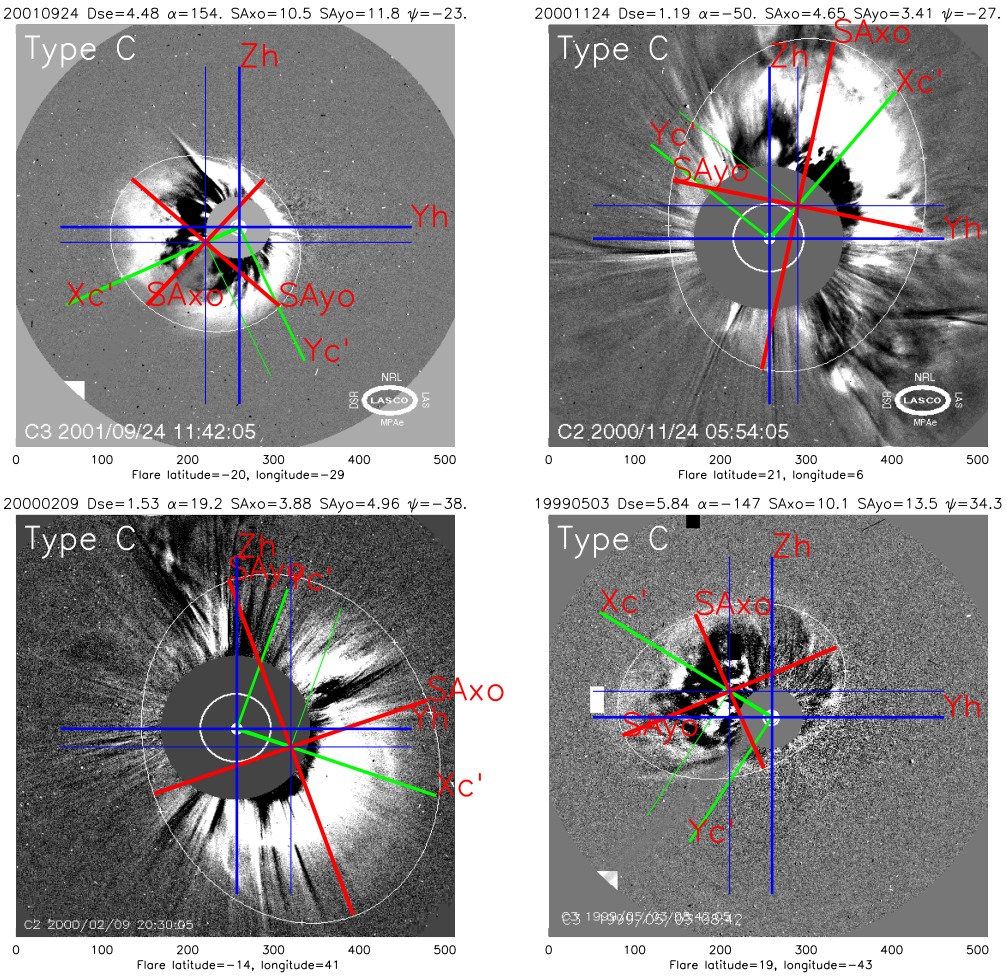

Fig. 3.— The four Type C halo CMEs studied in Zhao08, of which three cannot be reproduced using the inversion equation system in Zhao08. The measured values of the five halo parameters, ψ, α, SA_{xo}, SA_{yo}, and D_{se} are shown on the top of each panel. The heliographic latitude and longitude of associated flares are shown on the bottom of each panel.

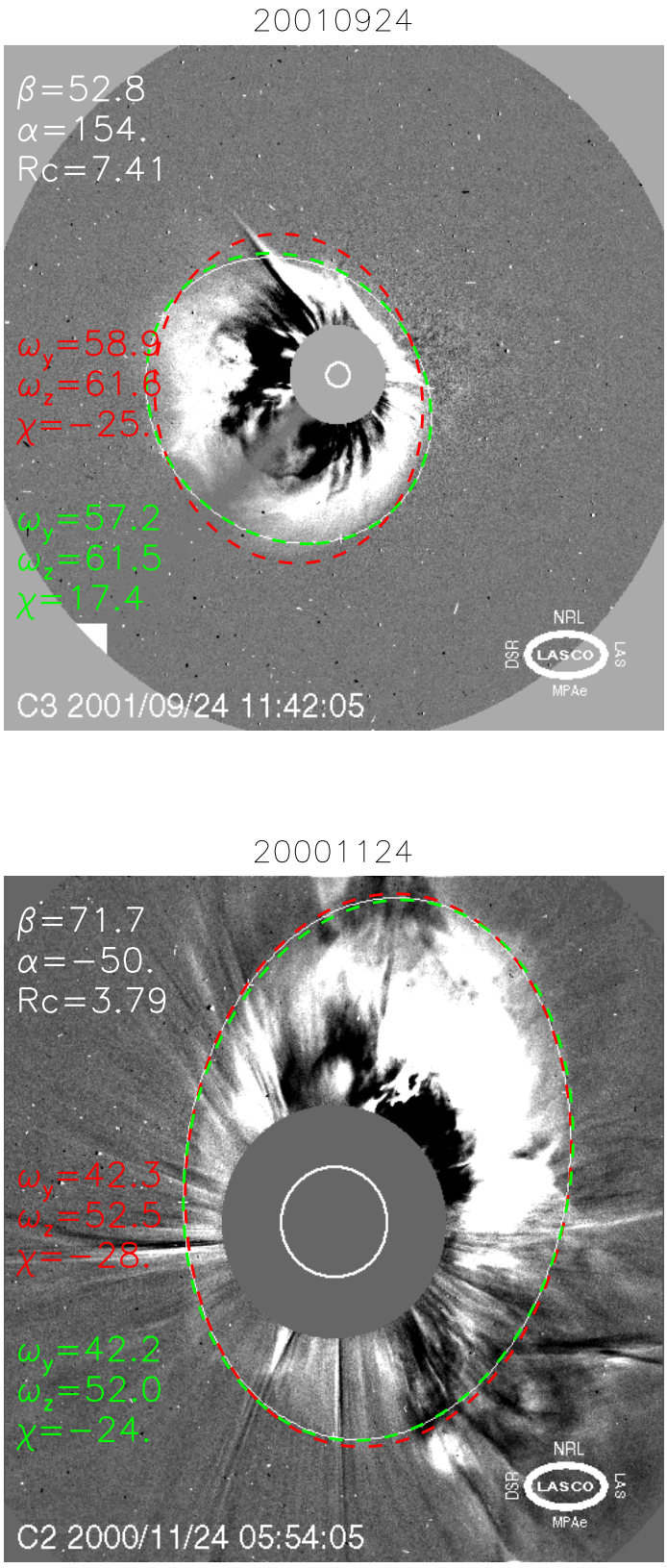

Fig. 4.— Comparison of modeled halos produced using new (green dashed) and old (red dashed) inversion equation systems with FFH CMEs (white) observed 2001.09.24_11:42 and 2000.11.24_05:54.

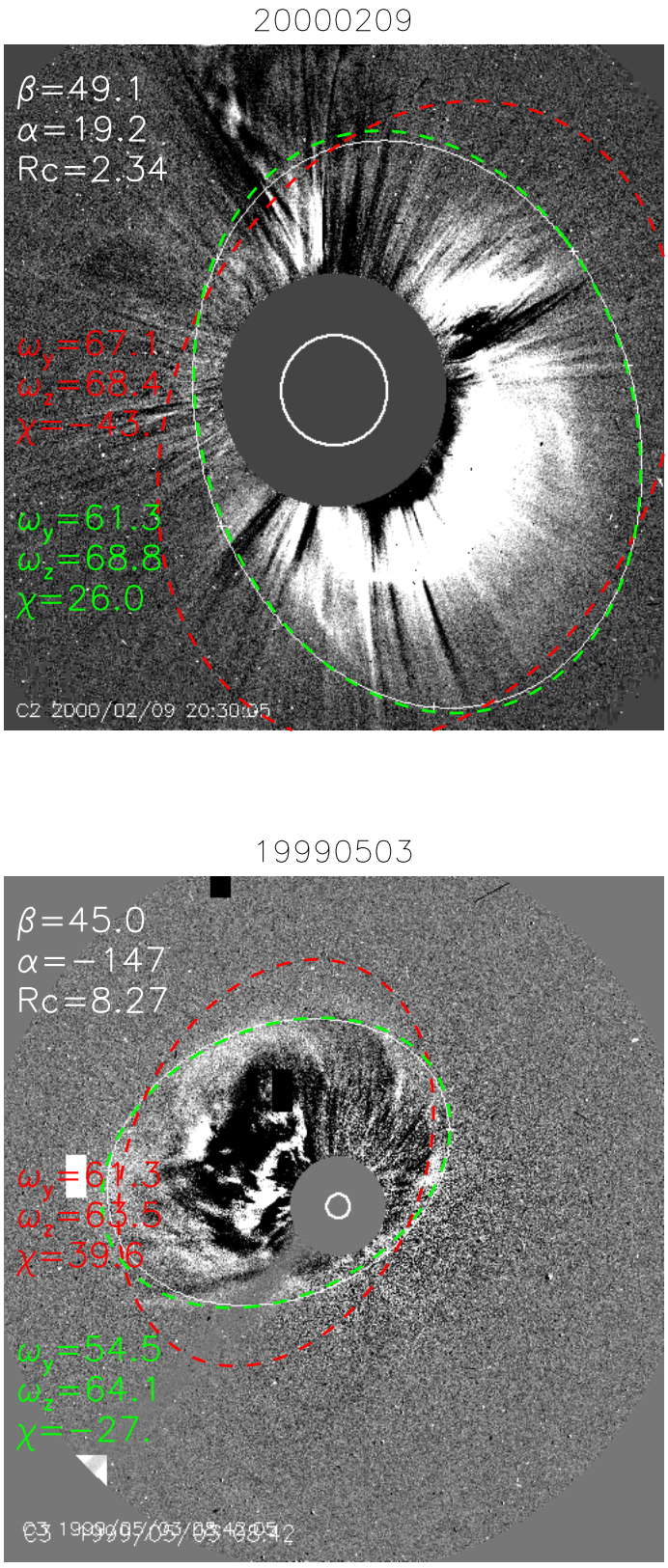

Fig. 5.— The same as Figure 4 but for 2000.02.09_20:30 and 1999.05.03_08:42.